Self-consistent model of hydrogen chemisorption on ferromagnetic transition metals

M. Streszewski* and C. Jędrzejek*
Department of Physics, Texas A&M University, College Station, Texas 77843-4242
(Received 2 December 1985; revised manuscript received 4 June 1986)

The chemisorption of hydrogen on ferromagnetic transition metals is studied self-consistently with use of a spin-dependent Anderson-Hubbard Hamiltonian. The electronic structure of the crystal is treated with the Bethe-lattice method. The present treatment differs from previous ones in that the dominant effects of the change in occupancy of the substrate orbitals are taken into account. The consequent modification of the substrate Hamiltonian leads to the result that the chemisorption energy changes very little with the change of the magnetization of the substrate. This finding agrees with recent experimental evidence that a magnetic phase transition has no influence on the catalytic activity.

I. INTRODUCTION

The chemisorption of hydrogen on transition metals is one of the most studied processes in surface science. One reason is that atomic hydrogen is directly involved in many chemical reactions at surfaces important in catalysis. Also, hydrogen is the simplest adsorbate, serving to test the general trends and mechanisms of chemisorption.

One of the most interesting problems is how hydrogen chemisorption affects the surface magnetization, and how the energy of chemisorption changes with substrate magnetization. A number of experimental studies addressed the second question, beginning with the observation of Hedvall fifty years ago,[1] of a "magneto-catalytic effect." Among the recent studies where different activation energies were observed in paramagnetic and ferromagnetic states is a change of the hydrogenation of ethylene over Ni-Cu alloys.[2] Similarly, Shanabarger[3] reported different activation energies above and below the Curie temperature T_C in the isothermal desorption kinetics of H_2 on polycrystalline Ni films. Also, Kaarmann *et al.*[4] found that the desorption rate of atomic hydrogen from Ni(110) is lower for the magnetized ($B=0.1$ T) than for the demagnetized surface. There is, however, strong evidence in the studies by Ertl and collaborators[5,6] that the change of chemical activity at the Curie temperature is caused by carbon impurities. Their measurements with rigorously clean surfaces produced no anomaly at T_C for decomposition of NH_3 on Ni,[5] or for dissociative hydrogen adsorption on Ni(111) and Ni(110).[6] Moreover, they revealed that if the surface was not clean enough spurious amounts of carbon were on the surface which dissolved into the bulk at T_C. Since carbon is a strong poison, its presence below T_C decrease catalytic activity.

Although the methods of magnetizing the surface were different in Refs. 5 and 6 than in Ref. 4, where the field was applied, the result of these two works dealing with the same system clearly are contradictory. In particular, in Ref. 4 the difference of activation energies in the magnetized and demagnetized states was shown to decrease with the increase of carbon coverage.

The activation or reaction energies studied experimentally are all related to the energy of chemisorption. The question whether the chemisorption energy is changed upon magnetization has not been addressed yet by first-principles methods, although the state of the art LSDA (local-spin-density approximation) calculations[7] are capable of providing a reliable answer. To give an estimate of the accuracy of LSDA we refer to Weiner and Davenport[7] who obtained a cohesive energy of 3.2 eV per H atom for $p(1\times1)$ monolayer of H on Hi(001), which is approximately 0.5 eV larger than the experimental value. For comparison, spin-unpolarized calculations of Umrigar and Wilkins[8] using the local-density-approximation (LDA) method for seven-layer slabs, consisting of five layers of Ni with a layer of H on each side, gave a chemisorption energy 3.61 or 3.42 eV, depending on an exchange-correlation potential used. In the same calculations, the chemisorption energy for the center hydrogen position is 0.32 eV lower than in the top position. This is in marked contrast with the generalized valence-bond calculations of Upton and Goddard,[9] who obtained a 1.48 eV difference of chemisorption energies between the same positions. The large difference between the last two calculations can probably be attributed to inaccuracies of the generalized valence-bond (GVB) model (as inferred from discussions on Cr and Mo dimers).[10]

In this paper we will study a hydrogen chemisorption using a self-consistent Anderson-Hubbard Hamiltonian. The Anderson-Hubbard Hamiltonian[11] has well-known deficiencies. The most important is not taking fully into account the role of s electrons[12,13] which, as was indicated by ultraviolet photoelectron spectra (UPS), might be important for the binding of H on Ni.[14,15] Part of the spin-polarization effects, such as the s-electron-mediated Ruderman-Kittel-Kasuya-Yosida (RKKY) interaction, are lost in this model. However, this method is capable of accounting for d-electron spin-polarization effects. Such effects clearly show the inadequacy of using doubly occupied spin orbitals (traditionally employed in the majority of textbooks and experimental papers), arising from the use of unpolarized quantum-chemical methods. Also, the method allows for treatment of a large class of different systems, and for explaining trends in the chemisorption energies of hydrogen on transition metals. In this respect, the method is similar to other simple calculational models of varying degrees of sophistication, such as the jellium

model,[16,17] effective medium approach,[18] and the methods of Varma and Wilson[19] or Baetzold and Shustorovich.[20]

Spin polarization effects were studied by Bell and Madhukar,[21] Kranz,[22] and Oleś and Chao.[23] In particular, Morán-Lopéz and Falicov[24] solved the Anderson-Hubbard Hamiltonian (the model obtained by including Coulomb interactions on crystal atoms in the Newns model), in the Hartree-Fock and Bethe-lattice approximations, and concluded that the energy of chemisorption changes substantially upon the change of magnetization.

In this paper we use essentially the Morán-Lopéz and Falicov formalism, but with a very important extension. We treat self-consistently not only the occupation numbers of the hydrogen and the substrate d states directly coupled to the hydrogen, but also the rest of the d orbitals at the substrate surface.

Our results show a very weak dependence of the chemisorption energy on the magnetic parameters of the substrate, which is in agreement with the experimental results of Ertl and collaborators. Also, contrary to the prediction of Ref. 24, the magnetic moment on the substrate is significantly reduced, in better accord with the experimental observations of Landolt and Campagna[25] and the theoretical "first principle" calculations of Weinert and Davenport.[7]

II. FERROMAGNETIC SUBSTRATE

To describe a ferromagnetic metallic substrate, we use the Hubbard Hamiltonian[26]

$$H_m=\sum_{i,j;\alpha;\sigma} t_{ij}c^{\dagger}_{i,\alpha\sigma}c_{j,\alpha\sigma}+\sum_{i;\alpha,\beta} U_{\alpha\beta}c^{\dagger}_{i,\alpha\downarrow}c_{i,\alpha\downarrow}c^{\dagger}_{i,\beta\uparrow}c_{i,\beta\uparrow}\ , \tag{1}$$

where the $t_{ij}=t$ are the hopping integrals between two neighbor sites i and j, σ is the spin index, $U_{\alpha\beta}=U$ are intrasite Coulomb interactions, α and β are orbital indexes ($\alpha,\beta=1,2,\ldots,5$), and $c^{\dagger}_{i,\alpha\sigma}$, and $c_{i,\alpha\sigma}$ are creation and annihilation operators in a Wannier space. It is assumed here that all five d bands are degenerate and have the same occupation in the bulk. Although great effort has been devoted to the studies of the Hubbard model,[27–29] the exact properties of its ground state are not known for two- and three-dimensional systems. The s states are only partly accounted for. It is assumed that they can be divided into two groups: (i) those within the energy range of the d bands with a width roughly 5 eV, and (ii) those beyond this range, which constitutes the rest of the s band extending over roughly 10 eV. The group (i) s states hybridize with the d states, forming an effective d band and contributing a part of the s electrons to this band, as reflected by nonintegral d-band occupation n in Table I. The s electrons are also implicitly taken into account by a drastic screening of otherwise large Coulomb interaction U.

In the unrestricted Hartree-Fock (UHF) approximation the Hamiltonian (1) can be rewritten in the form[11]

$$H_m=\sum_i\left[\sum_{\alpha,\sigma}\left(\sum_j t_{ij}c^{\dagger}_{i,\alpha\sigma}c_{j,\alpha\sigma}+U\langle n_{i,\bar{\sigma}}\rangle n_{i,\alpha\sigma}\right)-U\langle n_{i,\uparrow}\rangle\langle n_{i,\downarrow}\rangle\right], \tag{2}$$

where $\langle n_{i,\sigma}\rangle$ denotes the total number of electrons of spin σ at site i, and $\bar{\sigma}$ is the spin index opposite to σ. All occupation numbers in this approximation must be self-consistent. This means that the average number of electrons with spin σ at each site i calculated by use of the Hamiltonian (2) must be the same as that which is put into this Hamiltonian. Using the Bethe-lattice method[30,31] it has been shown[28] that, depending on the scaled Coulomb repulsion (U/W), where W is half of the d-band width, and on the electron concentration n, the ground state can correspond to a Pauli paramagnet, a ferromagnet, an antiferromagnet, or a ferrimagnet. Since the Hartree-Fock approximation and most of its improvements are far from exact, the above statement is subject to an uncertainty shared by the majority of models of interacting electrons with short-range interactions. The $\langle n_{i,\sigma}\rangle$ can be different for spins $\uparrow$ and $\downarrow$ and they are independent on the site index i. In the ferromagnetic case $\langle n_{i,\sigma}\rangle=n_{\sigma}$, whereas in the paramagnetic case $\langle n_{i,\sigma}\rangle=n$. This relatively crude assumption that the surface atoms have the same occupation numbers as the bulk atoms comes from the Bethe-lattice approximation, and it is made to decrease the number of parameters in the self-consistent scheme.

The self-consistency of the Hamiltonian (2) can be written now as the following set of equations:

$$n_{\sigma}=\int_{-\infty}^{E_F}\rho_{\sigma}(\omega)d\omega\ , \tag{3}$$

TABLE I. Input parameters used in the calculation of the properties of three substrates in their paramagnetic (PM) and ferromagnetic (FM) states, and self-consistent values of occupation numbers $n_{i\alpha\sigma}$, magnetic moment μ, and Fermi level E_F. In all cases the half of the bandwidth $W=2$ eV.

Case		z	U	n[a]	$n_{i\alpha\uparrow}$	$n_{i\alpha\downarrow}$	μ[b]	E_F
bcc Fe	PM	8	0.760	7.7	0.770	0.770	0.000	3.902
	FM	8	0.760	7.7	0.958	0.582	1.881	3.935
fcc Fe	PM	12	0.760	7.7	0.770	0.770	0.000	3.967
	FM	12	0.760	7.7	0.968	0.572	1.980	3.925
fcc Ni	PM	12	1.016	9.4	0.940	0.940	0.000	6.390
	FM	12	1.016	9.4	0.996	0.884	0.531	6.435

[a] $n=n_{i\uparrow}+n_{i\downarrow}$.

[b] $\mu=5(n_{i\alpha\uparrow}-n_{i\alpha\downarrow})$.

where

$$\rho_\sigma(\omega)=-\frac{5}{\pi}\mathrm{Im}G_{0\alpha,0\alpha;\sigma}(\omega;n_{\bar\sigma}) \tag{4}$$

is the density of the states at site i and for spin σ at energy ω. $G_{i\alpha,j\beta;\sigma}$ is the Green's function of the spin-σ electron connecting sites i and j and orbitals α and β, respectively. The Fermi energy E_F is chosen in such a way to keep the total number of electrons

$$n_\uparrow+n_\downarrow=n \tag{5}$$

constant.

In the Bethe-lattice approximation, the diagonal one-particle Green's function $G_{0\alpha,0\alpha;\sigma}$ has the following form:

$$G_{0\alpha,0\alpha;\sigma}(\omega;n_{\bar\sigma})=\frac{1}{\omega-\varepsilon_0^\sigma-zt\gamma^\sigma}\ , \tag{6}$$

where $\varepsilon_0^\sigma=Un_{\bar\sigma}$, z is the topological factor which represents the number of nearest neighbors in the Bethe lattice for each site, and

$$\gamma^\sigma=\frac{(\omega-\varepsilon_0^\sigma)-i[4(z-1)t^2-(\omega-\varepsilon_0^\sigma)^2]^{1/2}}{2(z-1)t}\ , \tag{7}$$

where γ^σ is the transfer matrix,[28] which describes the properties of the whole crystal, and, in particular, defines the position of the band region. Henceforth $n_{a\sigma}^0$ and $n_\sigma^0=5n_{a\sigma}^0$ will refer to the pure crystal, and $n_{a\sigma},n_\sigma$ will represent the system in the presence of the adatom-lattice interaction.

III. CHEMISORPTION MODEL

Using the ideas of Anderson[32] and Newns,[11] we can now introduce a hydrogen atom into the Hamiltonian by including a hopping integral t_a. Following Ref. 24 we may write the chemisorption Hamiltonian in the UHF approximation as

$$H=H_m+\sum_\sigma(E_a+U_a\langle n_{a\bar\sigma}\rangle)c_{a\sigma}^\dagger c_{a\sigma} +t_a(c_{a\sigma}^\dagger c_{0,1\sigma}+c_{0,1\sigma}^\dagger c_{a\sigma})-U_a\langle n_{a\uparrow}\rangle\langle n_{a\downarrow}\rangle\ , \tag{8}$$

where U_a is the intra-atomic Coulomb interaction energy of the hydrogen atom, whereas the hopping integral t_a connects the adatom electronic states and one orbital of proper symmetry (labeled 1) of the substrate atom at site 0 only (see Ref. 24).

A schematic picture of an adatom near metallic surface is presented in Fig. 1. The hybridized d and s states form roughly a 5-eV band. The work function is of approximately the same size. The atomic level of hydrogen, -13.6 eV, lies well below the bottom of the d band. Neglecting the adatom-crystal interaction, if the second electron is added to the adatom it will have an energy E_a+U_a. In the case of hydrogen, E_a+U_a is the negative of the electron affinity, which is about 0.7 eV. This level lies above E_F. To include a polarization effect due to the neglected core electrons (and part of the $4s$ states) of the transition-metal atoms, we will use effective E_a and U_a values. The choice of these parameters will be discussed in the next section.

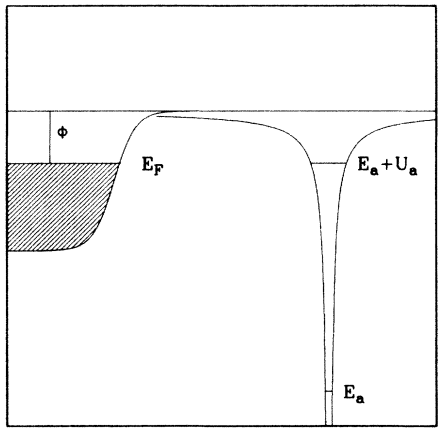

FIG. 1. Schematic picture of noninteracting hydrogen near a transition-metal surface.

Before we write down the equations for the Green's function, which we shall use to derive formulas for the number of electrons, we would like to make some comments: The Hamiltonian (8) can be written in the form

$$H=H_0+H'(t_a)\ , \tag{9}$$

where $H'(t_a)=0$ for $t_a=0$. It may appear[24] that

$$H'(t_a)=t_a\sum_\sigma(c_{a\sigma}^\dagger c_{0,1\sigma}+\mathrm{H.c.})\ ,$$

but this is not the case.[31] For $t_a=0$

$$H=H_0=H_m(n_{i,a\sigma}=n_{i,a\sigma}^0)+E_a c_{a\sigma}^\dagger c_{a\sigma}\ , \tag{10}$$

where $\sigma=\uparrow$ when the direction of the adatom spin is the same as the direction of the magnetic moment of crystal atoms, or alternatively $\sigma=\downarrow$ when the directions are opposite.

When we turn on the interaction between the adatom and the ferromagnetic substrate, the occupation numbers for the electrons will change both at the hydrogen and at the substrate atoms for all five orbitals. The change will produce an additional "impurity" inside the crystal.[31] However, we may expect that the change should decrease with increasing distance between the site 0 and given site i. In our approximation we restrict ourselves to the case when only the change in the number of electrons at the adatom and at the site 0 substrate atom is taken into account. Then H' can be written in the form

$$H'=\sum_\sigma\left[t_a(c_{a\sigma}^\dagger c_{0,1\sigma}+c_{0,1\sigma}^\dagger ca\sigma) +\sum_{\alpha=1}^{5}U\langle\Delta n_{\bar\sigma}\rangle c_{0,a\sigma}^\dagger c_{0,a\sigma}+U_a\langle\Delta n_{a\bar\sigma}\rangle c_{a\sigma}^\dagger c_{a\sigma}\right] -U(\langle n_\uparrow\rangle\langle n_\downarrow\rangle-\langle n_\uparrow^0\rangle\langle n_\downarrow^0\rangle)-U_a\langle n_{a\uparrow}\rangle\langle n_{a\downarrow}\rangle\ , \tag{11}$$

where $\Delta n_\sigma=n_\sigma-n_\sigma^0$ and $\Delta n_{a\sigma}=n_{a\sigma}-n_{a\sigma}^0$. There are two cases here—$n_{a\downarrow}^0=1$, $n_\downarrow^0=0$ or $n_{a\uparrow}^0=0$, $n_\downarrow^0=1$—and both will be taken into account.

Using Dyson's equation for the perturbation H', one can find

$$G_{a,a;\sigma}(\omega)=\left[\omega-E_a^\sigma-\frac{t_a^2}{\omega-\varepsilon^\sigma-zt\gamma(\omega,\varepsilon_0^\sigma)}\right]^{-1},$$

$$G_{01,01;\sigma}(\omega)=\left[\omega-\varepsilon^\sigma-zt\gamma(\omega,\varepsilon_0^\sigma)-\frac{t_a^2}{\omega-E_a^\sigma}\right]^{-1},$$

$$G_{0\alpha,0\alpha;\sigma}(\omega)=\frac{1}{\omega-\varepsilon^\sigma-zt\gamma(\omega,\varepsilon_0^\sigma)}, \quad (12)$$

where $\alpha=2,3,4,$ and 5, and $E_a^\sigma=E_a+U_a\langle n_{a\bar{\sigma}}\rangle$, $\varepsilon_0^\sigma=U\langle n_{\bar{\sigma}}^0\rangle$, and $\varepsilon^\sigma=U\langle n_{\bar{\sigma}}\rangle$. The transfer matrix γ^σ is still the same as that which was defined by Eq. (7) (i.e., it still depends only on the parameters n_σ^0, not on n_σ or $n_{a\sigma}$).

There are two important facts which should be commented on here.

(i) The transfer function γ^σ has not been changed by the adatom, since the perturbation is local and does not affect the whole crystal. This means that the position of the band region is still the same as without the hydrogen atom. It follows from the formulas 3.2 through 3.8 in Ref. 24 that γ^σ depends on the adatom-crystal occupations $n_{i\alpha,\sigma}$ in whole system after the chemisorption. This assumption is not warranted even for a monolayer of hydrogen, and certainly not for a single H atom; rather it corresponds to the presence of a macroscopic number of hydrogen bulk impurities. Also, for the single adsorbate atom, the Fermi energy and the work function will not change upon the chemisorption. The situation is different for finite coverage of an adsorbate, since a polarization of the adsorbate may consequently change a work function, and positions of bands and localized states relative to the vacuum level.

(ii) While it seems that hopping integral t_a connects an adatom with the orbital 1 of the atom at site 0 only, the other four orbitals of that atom can indirectly participate in the charge transfer with the adatom because of the Coulomb interaction U in the Hamiltonian (2) of the crystal.

In Eq. (12) Green's functions $G_{a,a;\sigma}(\omega)$ and $G_{01,01;\sigma}(\omega)$ have the same residues. In the case of these functions, following the conclusion in Ref. 11, we may have a maximum of two localized states for each spin (one below and the other above the band, corresponding to bonding and antibonding states, respectively). Since $G_{0\alpha,0\alpha;\sigma}(\omega)$, $\alpha=2,3,4,5$ have different residues than $G_{a,a;\sigma}(\omega)$ and $G_{01,01;\sigma}(\omega)$ functions, we may obtain new (up to four) localized states for certain values of t_a and other parameters. We indeed find this to be the case in the calculations presented below. Due to the more complicated electronic structure in the present theory it is not possible to obtain completely analytic results.

IV. SCHEME OF CALCULATIONS

A. Choice of input parameters

The role of input parameters in our model is similar to these in semiempirical quantum chemistry methods, such as CNDO/2 (complete neglect of differential overlap) for example. It is widely recognized that the internal consistency of such theories demands that the basis wave functions not be interpreted as free-atom orbitals.

Below we give the motivation for the choice of t, U, t_a, U_a, and E_a. For Fe we use the same parameters as Morán-Lopéz and Falicov[24] in order to compare the predictions of two methods.[33] For all systems W, the half bandwidth is chosen to be 2 eV. With these parameters for the pure ferromagnetic substrate the width of d band agrees within 2% with the values taken from Watson and Bennet[34]—a whole bandwidth of 5.73 eV for Fe and 4.64 eV for Ni. Since we do not calculate the work function, but instead treat it as an input parameter, we have chosen the energy difference between the zero crystal level, when $U=0$, and the hydrogen atomic level as fixed. This causes the change of the position of the hydrogen atomic level with respect to the vacuum of at most 0.05 eV upon changing the magnetization of the substrate (as seen in Table I), which causes a negligible error.

With reference to the calculations of the properties of the ferromagnetic substrate, one cannot expect full internal consistency using the Hubbard model in the UHF approximation. HF theory consistently overestimates the tendency toward the magnetic instabilities due to the neglect of other correlation effects. To compensate for this one should use, instead of U, a smaller renormalized value U_{eff}, given by

$$U_{\text{eff}}=U(1+U/\gamma)^{-1},$$

where γ is of the order of the bandwidth.[35] Our values of $U_{\text{eff}}=0.76$ eV for Fe and $U_{\text{eff}}=1.016$ eV for Ni agree very well with $U=0.9$ eV for Fe and $U=1.32$ eV for Ni, based on the first-principles calculations and used by Hubbard[36] in his model of a randomized exchange field. Experimentally, for transition metals it is possible to determine the Coulomb interaction between two holes on the same site from the Auger spectra.[37] However, the two-hole onsite Coulomb interaction is not quite the Hubbard U, particularly for partially filled d bands. In determining the parameters related to the hydrogen atom, one expects the one-body picture to be even less valid than for the substrate. For the noninteracting hydrogen U_a calculated with exact $1s$ functions (when only one electron is present) is 17 eV. However, U_a determined from affinity equals $13.6-0.7=12.9$ eV. The presence of metal screening will cause a further decrease of U_a. The classical image effects of Lyo and Gomer,[38] and Einstein *et al.*[39] lead to an estimate of U_a of being as low as 6 eV. However, the classical image calculations strictly hold only at large distances from surface. Also, that estimate refers to U_a as the energy difference between the antibonding and bonding energy levels upon chemisorption, U_{chem}. Although one is allowed to use a renormalized U due to unaccounted effects (neglected core electrons and partly $4s$ states of transition metal atoms), one should not use U_{chem} as a parameter U in the Hamiltonian to avoid double-counting effects. To describe the adsorbate, as input parameters we use $U_a/W=5.16$ for all cases (the same value as used by Morán-Lopéz and Falicov as a compromise between the atomic value 12.9 and $U_{\text{chem}}=6$

eV) and $E_a/W=-3.0$ for bcc and fcc Fe, and $E_a/W=-1.1$ for Ni. These values E_a correspond to the atomic hydrogen level with respect to the vacuum, when the experimental values of the work functions 4.5 eV for Fe and 5.15 eV for Ni are used.[40] We neglected a shift of E_a due to unaccounted polarizations, since otherwise t_a, the adatom-surface coupling parameter, cannot be related to the adatom distance from the surface in a simple way. In our calculations all energies are chosen relative to the energetic scale of the Hamiltonian (8) (zero energy corresponds to the center of the band in case of zero occupation number of the substrate).

Bare values of the integrals t_a, t, U, and U_a may be calculated using their formal definitions. The second quantization operators introduced at the beginning of this paper are related to nonorthogonal basis sets. This was not important in our calculations since we have never used the anticommutation properties (in nonorthogonal basis):

$$\{c^{\dagger}_{a\sigma},c^{\dagger}_{\beta\sigma'}\}=\{c_{a\sigma},c_{\beta\sigma'}\}=0\ ,$$
$$\{c^{\dagger}_{a\sigma},c_{\beta\sigma'}\}=\delta_{\sigma\sigma'}S_{a\beta}=\delta_{\sigma\sigma'}\int\phi^{*}_{a}(x)\phi_{\beta}(x)d^{3}x\ .$$

The nonorthogonality becomes explicit in the definitions of the integrals t_a and t. Any one-particle operator, defined by use of field operators in second quantization scheme as

$$T=\int\Phi^{\dagger}(x)T(x)\Phi(x)d^{3}x\ ,$$

may be rewritten in a nonorthogonal basis in the form

$$T=\sum_{i,j,k,l}c^{\dagger}_{i}S^{\dagger-1}_{il}\langle l\mid T\mid k\rangle S^{-1}_{k,j}c_{j}\ , \tag{13}$$

where the summation goes through the whole nonorthogonal basis set. In most calculations using model Hamiltonians nonorthogonality is not accounted for. We will present our results as functions of the coupling parameter t_a. We have verified using Slater-type orbitals[41] that restricted Hartree-Fock method gives $t_a/W=1.6-1.8$ eV (in agreement with the estimate of Newns[11]) for the experimentally relevant H-Ni distances 1.75–1.90 Å.[7] For hydrogen on an Fe system we are not aware of any experimental determination of H-Fe distances. Taking the same range of distances 1.75–1.90 Å in on top geometry we obtained $t_a/W=1.1-1.4$. It is worth stressing that one would ultimately like to use the occupation dependent values of t_a and U_a, beyond the Hartree-Fock scheme. Using formula (6) and Eqs. (3), (4), and (5), we present in the Table I the values of the magnetic moment and Fermi energy obtained for three systems. The input parameters correspond, approximately, to bcc Fe, fcc Fe, and fcc Ni in their paramagnetic and ferromagnetic states. For calculations of chemisorption energies, we use the values of the occupation numbers n^{0}_{σ} and the Fermi energies as input substrate parameters.

B. Self-consistency scheme

In the presence of the adsorbate the equations for self-consistency can be written in the following form:

$$N[N(n_{\sigma})]=n_{\sigma},\quad \sigma=\downarrow,\uparrow\ , \tag{14}$$

where now both N and n_σ are three component vectors

$$n_{\sigma}=\begin{bmatrix}n_{a;\sigma}\\ n_{01;\sigma}\\ 4n_{0\alpha;\sigma}\end{bmatrix},\quad N(n_{\sigma})=\begin{bmatrix}N_{a}(n_{\bar\sigma})\\ N_{01}(n_{\bar\sigma})\\ N_{0\alpha}(n_{\bar\sigma})\end{bmatrix}, \tag{15}$$

where $\alpha=2,3,4$, or 5 and

$$N_{a}(n_{\bar\sigma})=-\frac{1}{\pi}\mathrm{Im}\int_{-\infty}^{E_F}G_{a,a;\sigma}(\omega;n_{\bar\sigma})d\omega\ ,$$
$$N_{01}(n_{\bar\sigma})=-\frac{1}{\pi}\mathrm{Im}\int_{-\infty}^{E_F}G_{01,01;\sigma}(\omega;n_{\bar\sigma})d\omega\ , \tag{16}$$
$$N_{0\alpha}(n_{\bar\sigma})=-\frac{4}{\pi}\mathrm{Im}\int_{-\infty}^{E_F}G_{0\alpha,0\alpha;\sigma}(\omega;n_{\bar\sigma})d\omega\ ,$$

where G is described by Eq. (12). The equations are coupled and nonlinear. Note that in case of the pure crystal we need to solve only one such nonlinear equation [see Eq. (3)], since all orbitals are described by the same equation. Now the adatom is described by the first component of the Eq. (14), the orbital 1 of the site 0 atom (which is directly connected to the adatom) is represented by the second component of the vector equation, and orbitals 2–5 are represented by the third component, respectively. It is worth noting that in previous calculations[24] only occupations of adatom and orbital 1 of the site 0 substrate atom were determined self-consistently. When neighboring atoms of the site 0 are taken into account, the set of self-consistency equations will become yet more difficult.

V. NUMERICAL RESULTS

The following results have been obtained from the numerical solution of the Eq. (14) for $t_a/W\in[0,2]$. The three main cases have been taken into account: (1) "fer-

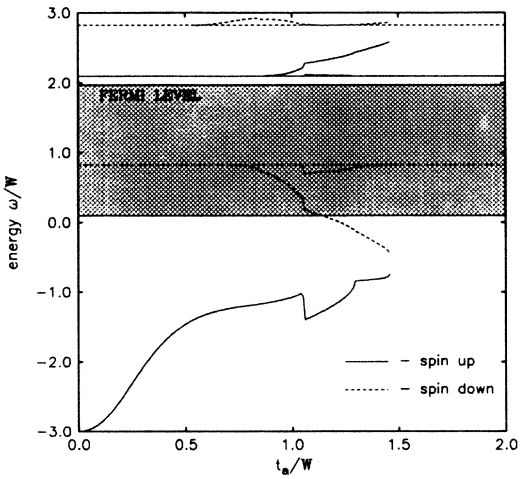

FIG. 2. The position of the localized states as a function of t_a/W for the "ferromagnetic" case of bcc Fe. Solid lines indicate spin-up states, and dashed lines spin-down states. The thick solid line is the Fermi level, whereas two pairs of thin straight lines (solid and dashed) correspond to the boundaries of the bands for spin up and spin down, respectively. The shaded region shows the occupied states.

romagnetic" case of chemisorption—when the initial (at $t_a=0$) polarization of the hydrogen electron spin is the same as the magnetic moment of the lattice, (2) "antiferromagnetic" case—when the polarization of the spin is opposite to the magnetic moment of the lattice, and (3) "paramagnetic" case—hydrogen chemisorption onto paramagnetic phase of the crystal.

In presenting numerical results, first we will analyze in detail the bcc Fe system. For the other two systems, fcc Fe and Ni, only the main results will be given, since they show trends similar to bcc Fe.

A. Position and spectral density of states

In our model, only that part of the substrate s states which hybridizes with the d band was taken into account by specifying a total number of electrons within the energy range of the d band. Since the rest of the s band was neglected, for finite t_a one can obtain localized states which fall outside the band. One may obtain positions and spectral density of localized states from Green's functions, as discussed in Sec. III. For any type of Green's function, depending on the number of zeros of its denominator, in general, one can find for each spin two, one, or no localized states. An inspection of Eq. (12) reveals two different denominators of the Green's functions for each value of the spin variable. Hence, in theory one can obtain up to eight localized states. In practice, for physical values of the input parameters, we observed up to six localized states for the ferromagnetic case and up to four localized states for the antiferromagnetic and paramagnetic cases. For fixed values of the other parameters, the number of localized states depends on a value of t_a corresponding to the adsorbate-surface distance. In addition to the localized states related to the s orbital of the hydrogen and the $3d$-orbital 1 of the site 0, compared to Ref. 24 the novel feature of our method is the appearance of new localized states associated with the orbitals 2–5 of the site 0 atom (see Fig. 2), resulting from including these orbitals in the self-consistency scheme. The discontinuities in the slope of the all shown quantities at certain values of t_a are related to the splitting of the adsorbate and substrate localized states from the bands.

In Fig. 2, we present the position of the localized states as functions of t_a/W for the ferromagnetic case. The thick solid straight line is the Fermi level, whereas two pairs of thin straight lines (solid and dashed) correspond to the boundaries of the bands for the spin-up and the spin-down electronic states. Solid lines show localized state positions for spin-up states, and dashed lines represent spin-down states. Figures 3 and 4 present the positions of localized states for the antiferromagnetic and paramagnetic cases.

To get a better understanding of the adatom-substrate interaction, the local density of states (LDOS) is presented for $t_a/W=0.4$, 1.0, and 1.3 both for the adatom [Figs. 5(a), 6(a), and 7(a)] and the substrate atom [Figs. 5(b), 6(b), and 7(b)] in the antiferromagnetic case. In these figures the short-dashed line corresponds to the LDOS of orbital 1 at site 0 directly interacting with the adsorbate; the long-dashed line represents LDOS of all other d orbitals together; and the thin solid line represents the total LDOS for the site 0 atom. The thick solid line represents the Fermi level, and the shaded region indicates the occupied states. The right-hand and left-hand parts of the figures correspond to up and down spins, respectively. The spectral weights of the localized states are given.

The localized states have a profound effect on all properties of the system. As seen from Fig. 5 for a small value of $t_a/W=0.4$, corresponding to the adatom far from the surface, only majority-spin (relative to the lattice magnetization) adatom continuous states develop. Contrary to the $t_a=0$ case, shown in the inset of Fig. 5, bands become asymmetric. Two discrete substrate states, nonexistent at $t_a=0$, appear. For $t_a/W=1.0$, in addition to the majority-spin adatom continuous states, minority-spin continuous adatom states also develop. The bonding minority-spin level begins to show at the bottom of the

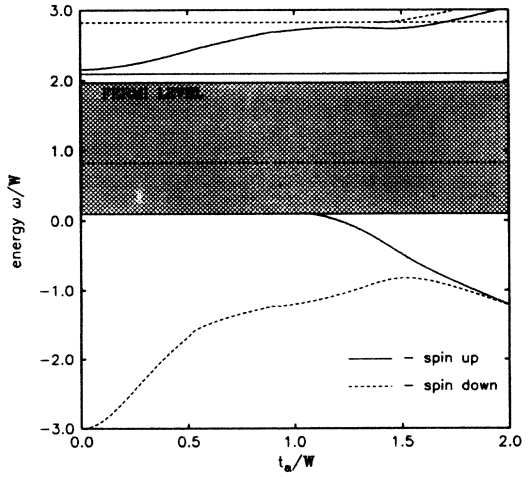

FIG. 3. The position of the localized states as a function of t_a/W for the "antiferromagnetic" case of bcc Fe. The labeling is the same as in Fig. 2.

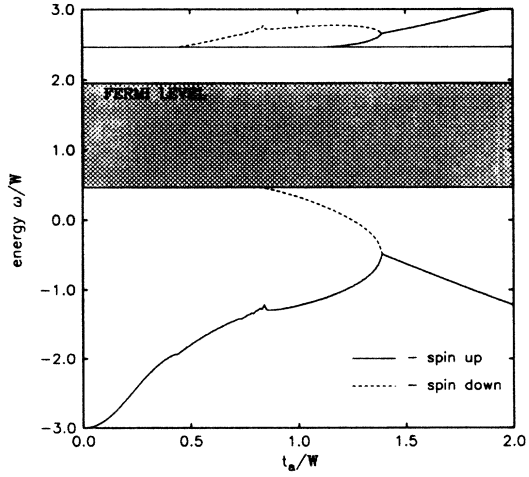

FIG. 4. The position of the localized states as a function of t_a/W for the "paramagnetic" case of bcc Fe. The labeling is the same as in Fig. 2.

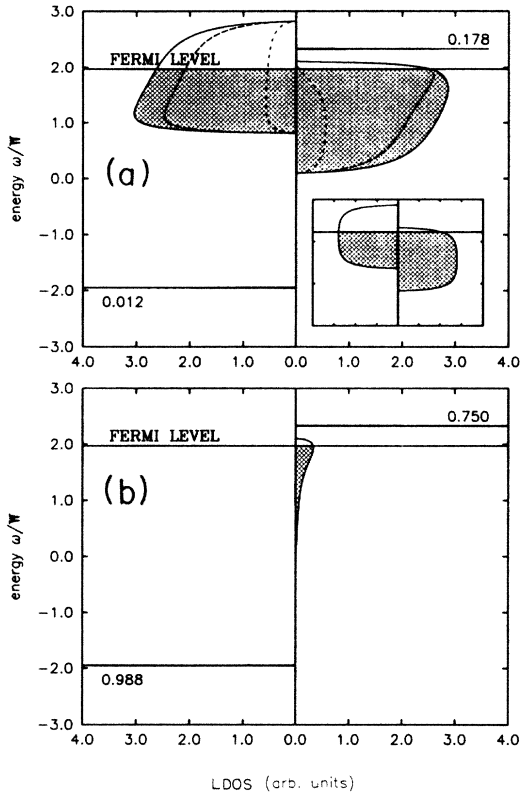

FIG. 5. The local density of states (LDOS) on the substrate atom (a) and on the adatom (b) for the "antiferromagnetic" case of bcc Fe with $t_a/W=0.4$. The thick solid line signifies the Fermi level, and the shaded region marks occupied states. Right-hand and left-hand parts of the figure correspond to up and down spins, respectively. The short-dashed line corresponds to the LDOS of orbital 1 at site 0. The long-dashed line represents the LDOS of all other d orbitals together, and the thin solid line represents the total LDOS for the site 0 crystal atom. The inset in the right corner displays the shape of the pure crystal band.

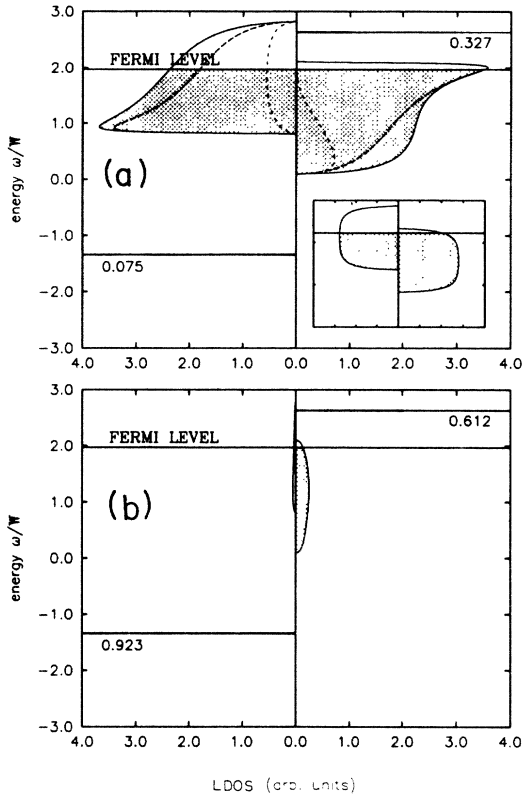

FIG. 6. The same as Fig. 5, but for $t_a/W=1.0$.

continuous band as seen in Fig. 6. The orbital 1 on the substrate is affected and is about to split. This splitting is completed at $t_a/W\approx 1.1$. As seen from Fig. 7, a peak at the top of the spin-down bands suggests the splitting of the localized state for slightly larger values of t_a.

B. Mechanism of adsorbate-surface interaction

We will now discuss the two major facts determining the mechanism of H-substrate interaction in this model.

1. Nonapplicability of spin-unpolarized perturbation theory

Due to the presence of Coulomb interactions, both on adatom and substrate the process of bonding *cannot* be described in terms of the simple spin-unpolarized second-order perturbation-theory results, the mainstay of chemical thinking, which states that two interacting levels pro-

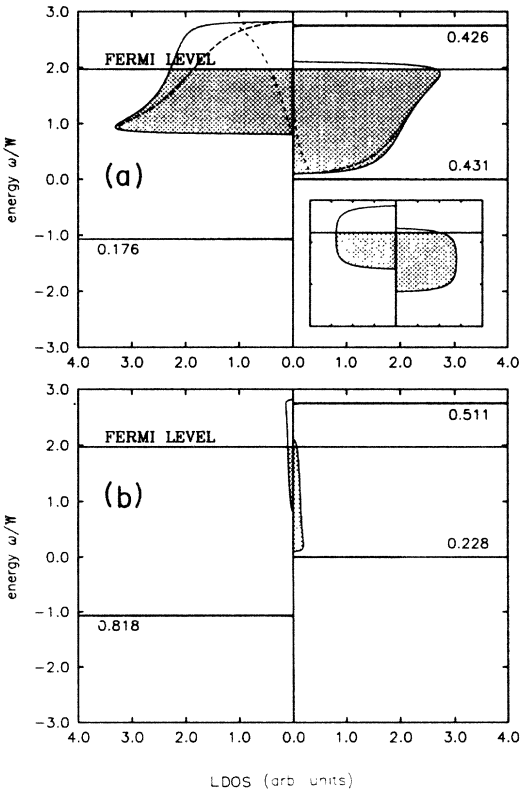

FIG. 7. The same as Fig. 5, but for $t_a/W=1.3$.

duce a lower-lying bonding molecular level and a higher-lying antibonding molecular level. Instead, one must distinquish between spin-up and spin-down states, as will be discussed for the antiferromagnetic case. The localized bonding minority-spin hydrogen state does not lower its energy upon switching on t_a. One can see this by analyzing the denominator of Green's functions $G_{a,a;\sigma}(\omega)$ and $G_{01,01;\sigma}(\omega)$

$$(\omega-E_a^\sigma)\left[\omega-\varepsilon^\sigma-\frac{z}{2(z-1)}\{\omega-\varepsilon_0^\sigma-[(\omega-\varepsilon_0^\sigma)^2-4(z-1)t_a^2]^{1/2}\}\right]-t_a^2 . \tag{17}$$

Outside the band, when $(\omega-\varepsilon_0^\sigma)^2 \gg 4(z-1)t_a^2$, zeros of the above expression are given by

$$(\omega-E_a^\sigma)(\omega-\varepsilon^\sigma)-t_a^2=0 . \tag{18}$$

This corresponds to the secular equation for the following two-level Hamiltonian:

$$H_{ij}^\sigma=\begin{bmatrix} E_a^\sigma & t_a \\ t_a & \varepsilon^\sigma \end{bmatrix} . \tag{19}$$

For small values of $t_a[4t_a^2<(\varepsilon^\sigma-E^\sigma)^2]$ the eigenvalues of this equation are

$$\begin{aligned} \varepsilon_1&=\tfrac{1}{2}\{E_a^\sigma+\varepsilon^\sigma+[(E_a^\sigma-\varepsilon^\sigma)^2+4t_a^2]^{1/2}\} \\ &=\varepsilon^\sigma+\frac{2t_a^2}{(\varepsilon^\sigma-E_a^\sigma)}+\cdots>\varepsilon^\sigma , \\ \varepsilon_2&=\tfrac{1}{2}\{E_a^\sigma+\varepsilon^\sigma-[(E_a^\sigma-\varepsilon^\sigma)^2+4t_a^2]^{1/2}\} \\ &=E_a^\sigma-\frac{2t_a^2}{(\varepsilon^\sigma-E_a^\sigma)}-\cdots<E_a^\sigma . \end{aligned} \tag{20}$$

Since $E_a^\sigma=E_a+U_a\langle n_{a\bar{\sigma}}\rangle$, then for small t_a,

$$U_a\langle n_{a\bar{\sigma}}\rangle>2t_a^2/(\varepsilon^\sigma-E_a^\sigma) ,$$

and consequently $\varepsilon_2>E_a$. This cannot happen for unpolarized calculations in which the term $U_a\langle n_{a\bar{\sigma}}\rangle$ does not apear. The binding comes about due to two facts: (i) There is a net decrease of the band center of gravity, and (ii) what was for $t_a=0$ the affinity hydrogen level becomes the majority-spin bonding state. This state acquires fractional occupation once the level is below the Fermi surface. (Also, the lowest state has an occupation number slightly smaller that 1 since, in general, the integral spectral density for this state decreases.) The majority-spin state is virtual while within the band and shifts down with the increase of t_a. The decrease of the chemisorption energy, due to the occupation of this level by electrons initially at the Fermi level, partly compensates the reverse effect related to the upward movement of the localized bonding minority-spin level. A correlation diagram explaining this mechanism is presented in Fig. 8. It is worth noting that once these two levels begin to converge, which happens for $t_a/W\approx 1.5$, above the experimentally relevant values of t_a for Fe, their occupation is approximately the same, and spin polarization plays a small role. Then, with the further increase of t_a both levels go down, and the standard chemical interpretation holds. With the change of terminology the above analysis holds also for the ferromagnetic and paramagnetic cases. For the paramagnetic case for $t_a/W>1.4$ spin-polarization plays no role.

The energy difference between the two lowest-energy states (having the opposite spin polarizations) can be considered as U_{chem}, and this quantity reflects the screening of $3d$ transition-metal states due to the presence of hydrogen. This quantity decreases with the increase of t_a and for large enough t_a becomes very small. It is also worth mentioning that a correct position of the lowest hydrogen level cannot be obtained by using a standard self-consistent restricted HF calculation (RHF). For a system like $HMn(CO)_5$ the RHF prediction of an energy of the lowest a_1 hydrogen level is not in agreement with the experimental results. Similar problems appear in the description of $Ni(C_3H_5)_2$, ferrocene, and other systems.[42]

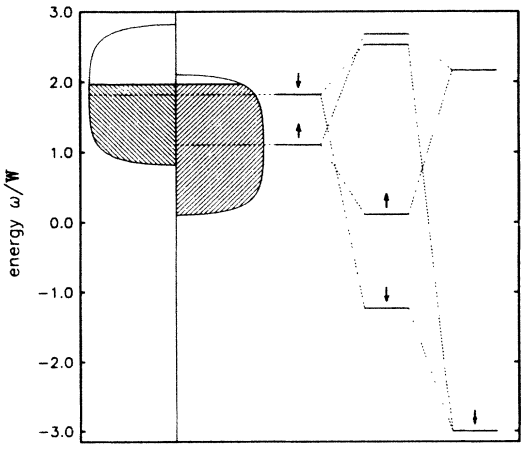

FIG. 8. Spin-dependent correlation diagram for H interacting with a transition-metal surface. The band of a given polarization is replaced by an effective level at the center of the band. In the range of $t_a/W<1.6$ for bcc Fe ($t_a/W=1.0$ at the diagram) the lowest hydrogen level moves up upon the chemisorption.

2. *Redistribution of density of states*

Since we consider a single adsorbate atom, the position of the bands and the exchange splitting are fixed. The Dyson's equation preserves the normalization, so the integrated density of states is not changed with a change of the coupling t_a. This refers to any state of a given spin in the absence of spin-flip interactions in the Hamiltonian (11). Consequently, the occupation of the majority (spin-up) bands and minority (spin-down) bands is determined by two factors: the change of the shape of the bands, and a division of the density of states between the band contribution and the contribution from the localized states. The increase of LDOS of the orbitals 2–5 at the bottom of the spin-down band, and at the top of the spin-up band, illustrates the important mechanism of the substrate demagnetization, due to the indirect coupling of adsorbate with these orbitals. Note that this mechanism prevails over the reverse trend for the orbital 1 as seen in Figs. 5–7. Equally important is a distribution change of the density of states (equal to the occupation numbers) for the localized states below the Fermi level, whose positions were shown in Fig. 3. This is illustrated in Fig. 9. The total occupation of the lowest (spin-down) localized state, on the adsorbate and the substrate, is almost constant as a function of t_a, and is approximately equal to 1. However, the occupation number on the substrate increases at the expense of the occupation number on the adsorbate. Once the second localized state, which is reversely polarized with respect to the lowest state, splits off the band, its total occupation number increases and tends to 1 for large t_a. In this limit, corresponding to the restricted Hartree-Fock case, the occupation numbers for both states become equal, both on the adsorbate and on the substrate. For $t_a \approx 1.3$, the total occupation number of the localized states below the Fermi level $n_{\rm loc}=(n_a+n_{01})_{\rm loc}\approx 1.8$ increases significantly compared to the $t_a=0$ case, when $n_{\rm loc}=1$. Since this correlates with the corresponding decrease of the continuous density of states for the level 1 at site 0 (see Figs. 5–7), this mechanism is important for the increase of the chemisorption energy. The main part of bonding comes from localized states.

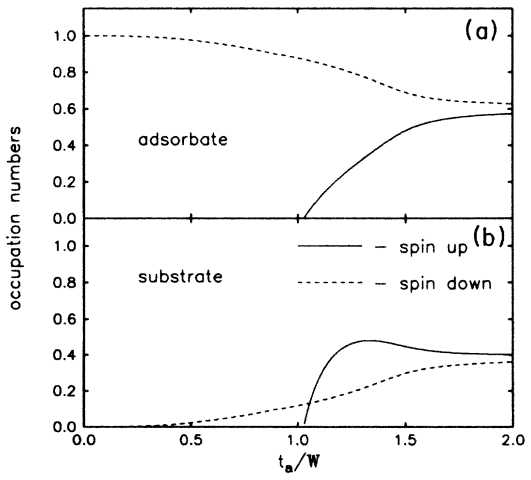

FIG. 9. Occupation numbers for the localized states below the Fermi level, whose positions are shown in Fig. 3. Solid lines indicate spin up states, and dashed lines spin down (minority-spin relative to the substrate), the lowest-energy states.

C. Charge transfer, magnetization, and chemisorption energy for hydrogen on bcc Fe

From the present model, one in principle could calculate the charge and spin densities. The space density of charge can be calculated if we include nondiagonal elements of the Green's function $G_{ij\sigma}(\omega)$. It turns out that in a nonorthogonal basis set of wave functions $\phi_k(x)$,

$$\rho^{\sigma}(\mathbf{x}) = -\mathrm{Im}\int d\omega \int d^3x'\,\delta^3(\mathbf{x}-\mathbf{x}')G_{\sigma}(\mathbf{x},\mathbf{x}';\omega) = \sum_{k,l,m}\phi_k^*(\mathbf{x})S_{kl}^{-1}\rho_{lm}^{\sigma}\phi_m^*(\mathbf{x})\ . \tag{21}$$

Here ρ_{lm} is density matrix in the atomic orbital basis

$$\rho_{lm}^{\sigma} = -\mathrm{Im}\int d\omega\, G_{lm;\sigma}(\omega)\ , \tag{22}$$

and

$$S_{kl} = \int d^3x\,\phi_k^*(\mathbf{x})\phi_l(\mathbf{x})$$

is the overlap matrix.

The charge transfer to the adatom is at the expense of the substrate. Most of it is from the first layer. Due to the very limited size of the quasimolecule we used, explicitly taking only the first layer, our method of embedding the quasimolecule though the Bethe-lattice approach does not allow us to determine the spatial distribution of the charge outside the quasimolecule. Therefore we do not attempt here to determine the dipole moments and the work functions, restricting ourselves to site charge transfer and magnetization.

The electron chemisorption energy can be calculated from

$$\Delta E = \sum_{\sigma}\int_{-\infty}^{E_F}(\omega-E_F)\rho_{a;\sigma}(\omega)d\omega-(E_a-E_F) + \sum_{\sigma\alpha}\int_{-\infty}^{E_F}(\omega-E_F)[\rho_{0\alpha;\sigma}(\omega)-\rho_{0\alpha;\sigma}^{0}(\omega)]d\omega - U_a\langle n_{a\uparrow}\rangle\langle n_{a\downarrow}\rangle - U[\langle n_{0\uparrow}\rangle\langle n_{0\downarrow}\rangle-\langle n_{0\uparrow}^{0}\rangle\langle n_{0\downarrow}^{0}\rangle]\ . \tag{23}$$

Equation (23) neglect partly the effect of 4s electrons on the transition-metal atoms and a polarization of the core electrons due to the hydrogen. In Figs. 10–12 we show detailed results for bcc Fe. We start with the magnetic moment of the adatom. $\mu_a=n_{a\uparrow}-n_{a\downarrow}$, the atom below at site 0, $\mu_0=n_{0\uparrow}-n_{0\downarrow}$, and the total magnetic moment of the quasimolecule consisting of the adatom and the surface atom at site 0, $\mu_{\rm tot}=\mu_a+\mu_0$ (Fig. 10). The ferromagnetic, antiferromagnetic, and paramagnetic cases are represented by the solid, long-dashed, and short-dashed lines, respectively. As we can see, the paramagnetic case has a nonzero magnetic solution in the range $0\le t_a\le t_{ac}$, $t_{ac}/W\approx 1.4$. The ferromagnetic solution becomes unstable at $t_{ac'}\approx 1.45$ (at the point which terminates the solid line). The solution flips to the antiferromagnetic case for $t_a\le t_{ac'}$. This feature of a very small difference between

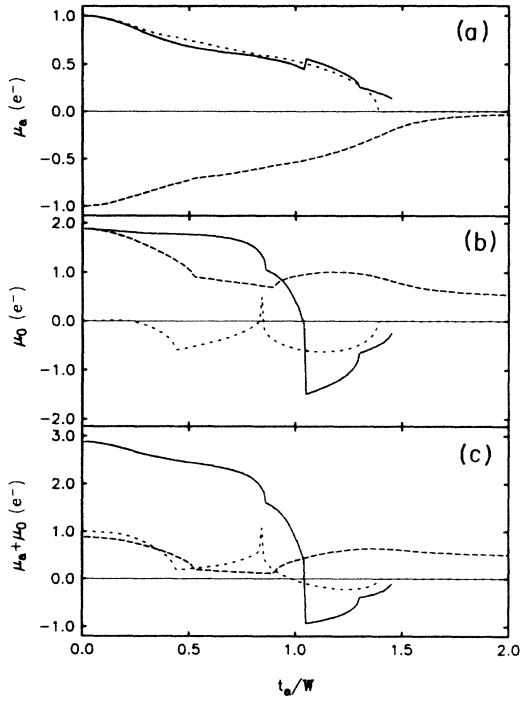

FIG. 10. Magnetic moment of the adatom μ_a, the atom below μ_0, and a quasimolecule μ_{tot} for bcc Fe. "Ferromagnetic," "antiferromagnetic," and "paramagnetic" cases (defined in the text) are represented by solid, long-dashed, and short-dashed lines, respectively.

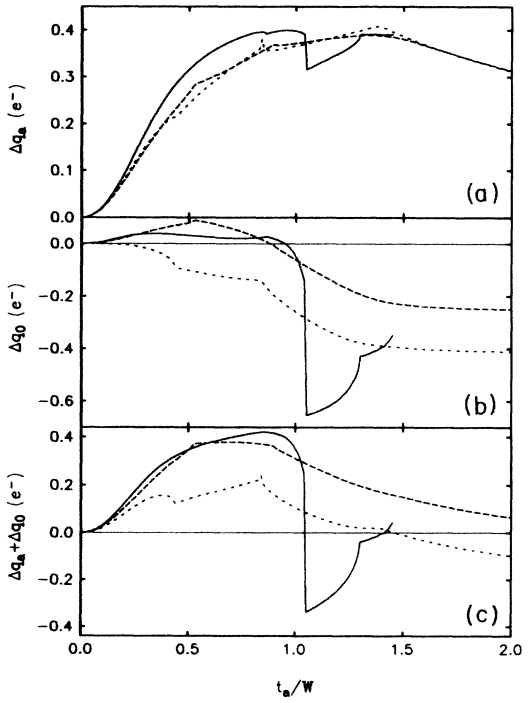

FIG. 11. The charge transfer on the adatom Δq_a, atom below Δq_0, and on the quasimolecule Δq_{tot}, in units of the number of electrons for bcc Fe. The meaning of the lines is as in Fig. 2.

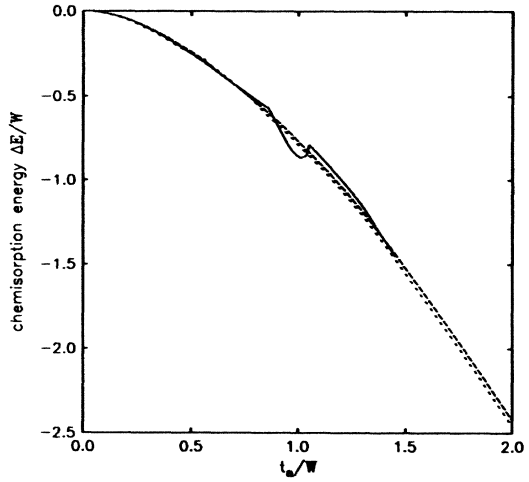

FIG. 12. The chemisorption energy in units of W as a function of t_a/W, for bcc Fe. Labeling is the same as in Fig. 2.

t_{ac} and $t_{ac'}$ is maintained for all cases we investigated.

In Fig. 11 the charge transfer is presented. Figure 11(a) shows $\Delta q_a = n_a - 1$, the net charge at the adatom; Fig. 11(b) presents $\Delta q_0 = n_0 - n$ ($n = 7.7$), the net charge at the atom below, whereas Fig. 10(c) shows the total net charge at the quasimolecule, $\Delta_q = \Delta q_a + \Delta q_0$. The labeling of the lines is the same as in Fig. 10. We can see in both Figs. 9 and 11 that, for the ferromagnetic case at $t_a/W \approx 1.05$, there is a sharp change in all these quantities. As seen in Fig. 12, the chemisorption energy is very weakly dependent on the magnetization of the substrate.

D. Comparison of the results of the present model with other theoretical results and experimental data

Due to the weak dependence of the Hamiltonian on the topological factor z ($\sim z^{1/2}$) the results for fcc Fe ($z = 12$) are qualitatively very similar to these for bcc Fe ($z = 8$). We present here only the charge transfer (Fig. 13) as an example.

We conclude the presentation of the numerical data with fcc Ni in Figs. 14–17, showing the magnetic moment (Fig. 14), charge transfer (Fig. 15), the local density of states of the adsorbate and substrate atom (Fig. 16), and the dependence of chemisorption energy on the coupling t_a (Fig. 17). In general the trends of behavior of the described properties for fcc Ni are similar to these of bcc and fcc Fe, although the values of the corresponding quantities are different.

For all systems studied, the dependence of the chemisorption energy on the magnetization state of the substrate is very weak. This result is in sharp contrast with the prediction of the Morán-Lopéz and Falicov[24] calculations. Allowing the polarization of all d orbitals in our method, absent in the previous calculational scheme,[24] might be partly responsible for the difference. The other, more important source of the discrepancy between the two calculations is related to the definition of the transfer function $\gamma^{\sigma}(\omega)$ given by Eq. (7). In our calculation scheme, $\gamma^{\sigma}(\omega)$ does not change upon the hydrogen chemisorption. It physically means that a single hydrogen

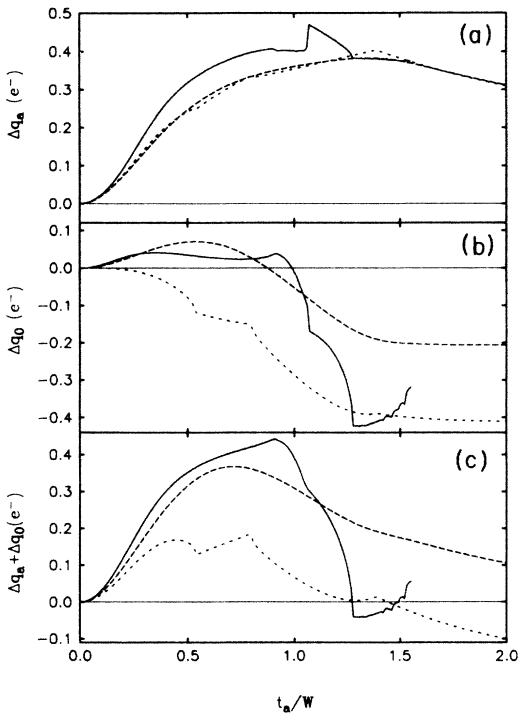

FIG. 13. The charge transfer on the adatom Δq_a, atom below Δq_0, and on the quasimolecule Δqtot in units of the number of electrons for fcc Fe. The meaning of the lines is as in Fig. 2.

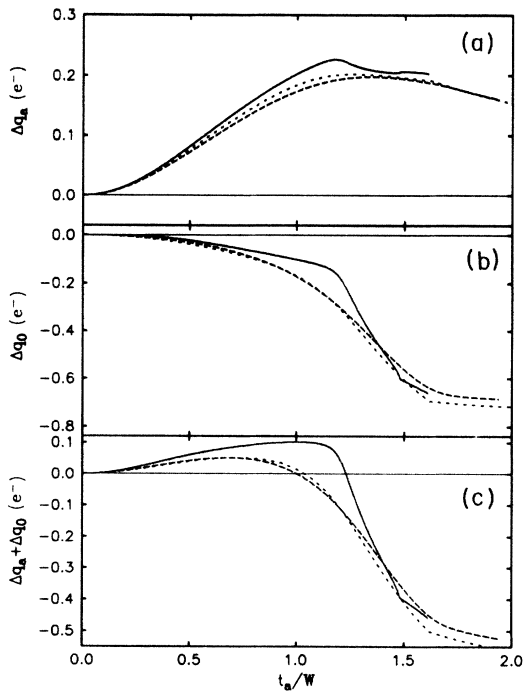

FIG. 15. The charge transfer on the adatom Δq_a, atom below Δq_0, and on the quasimolecule $\Delta q_{\rm tot}$, in units of the number of electrons for fcc Ni. The meaning of the lines is as in Fig. 2.

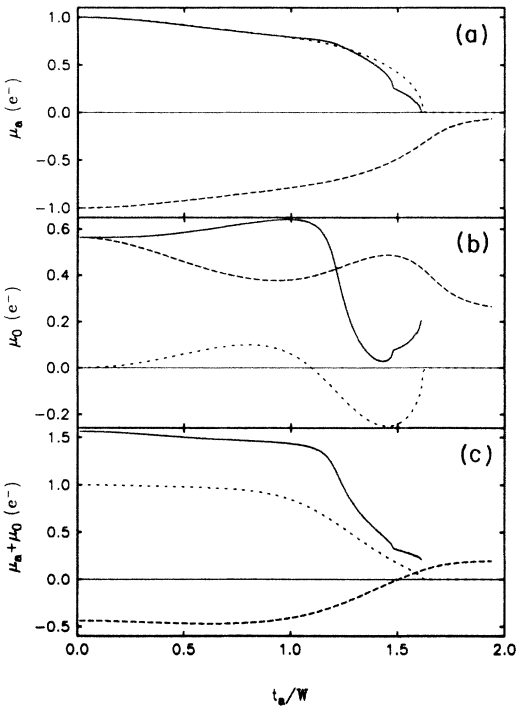

FIG. 14. Magnetic moment of the adatom μ_a, the atom below μ_0, and a quasimolecule $\mu_{\rm tot}$ for fcc Ni. Labeling is the same as in Fig. 2.

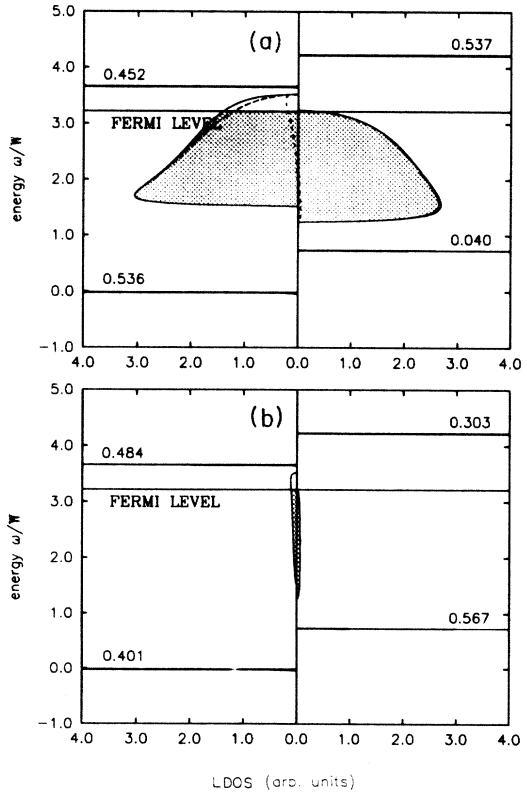

FIG. 16. The local density of states on the substrate atom (a) and on the substrate atom (b) for the "antiferromagnetic" case of fcc Ni with $t_a/W=1.0$. Labeling is the same as in Fig. 5.

atom cannot change the position of the band, so it does not move with respect to the vacuum.

For Fe and Ni hydrogen behaves as acceptor. The value of the charge transfer to hydrogen calculated by us for Ni ($\sim 0.1-0.2e$) is consistent with the value $\Delta q_a = 0.16e$ obtained by Newns[11] in his original paper. Our charge transfer for Fe ($\sim 0.3e$) is larger consistent with the trend observed by Newns, that the charge transfer decreases with the increase of the occupation of the d band. One consequence of the assumption that only d states of the transition metal are directly involved in binding might be too large a charge transfer to the hydrogen atom. In cluster calculations of H on Ni, including $4s$ states of Ni, Blyholder[43] obtained a charge transfer of less than $0.1e$, but it is not clear what is the effect of finite size of a cluster on charge transfer.

The magnetic moment of the substrate atom is significantly decreased upon chemisorption on ferromagnetic Fe in the relevant range of the coupling parameter $t_a/W = 1.1-1.4$. For Ni the effect exists, but is less pronounced in the relevant range of the coupling parameter $t_a/W = 1.6-1.8$. For this system, at $t_a/W \approx 1.7$, the chemisorption energy agrees very well with the experimental value -2.7 eV.[8] The demagnetization obtained in our calculations is smaller then experimentally observed[25] and calculated by Weineert and Davenport[7] for a monolayer coverage. It is to be expected that the demagnetization of the crystal atom in the presence of the single adsorbate atom is smaller than for a monolayer. It is also worth noting that in the previous calculations, using the Newns-Anderson-Hubbard model,[24] no decrease of magnetic moment in the first surface layer was obtained, and our demagnetization mechanism comes from taking into account the other four $3d$ orbitals in the self-consistency scheme.

Due to the fact that the $4s$ states are only partly accounted for in our model,[44,45] we do not expect quantitative reproduction of the experimental photoelectron peaks. We do, however, get for Ni the main chemisorption-induced peak at 6.1 eV below the Fermi level for $t_a/W = 1.7$, compared to the experimental value of 5.8 eV for Ni(111).[14,15] The history of this peak illustrates how difficult it is to study hydrogen on Ni. In contrast to an initial interpretation that it is H-Ni bonding level at room temperature,[14,15] Himpsel *et al.*[46] demonstrated that it is instead an enhancement of transitions from an *sp*-type bulk Ni band. That would suggest that hydrogen forms a broad resonance with metallic states, rather than a splitoff level. However, very recently Eberhardt, Plummer, and collaborators[47] showed the existence of the hydrogen derived splitoff state at low temperatures. They suggest that this state may not be observed at room temperatures because H is in invisible subsurface site. These facts emphasize the limitations of a zero-temperature description of materials at finite temperatures. We are not aware of any photoemission studies of hydrogen on monocrystal Fe.

VI. CONCLUSIONS

In this paper we extended the Morán-Lopéz and Falicov model of hydrogen chemisorption on Fe and Ni. As the main result of our calculations, we find that the chemisorption energy does not depend very much on the magnetization state of the substrate, in agreement with recent measurements of Ertl and collaborators.

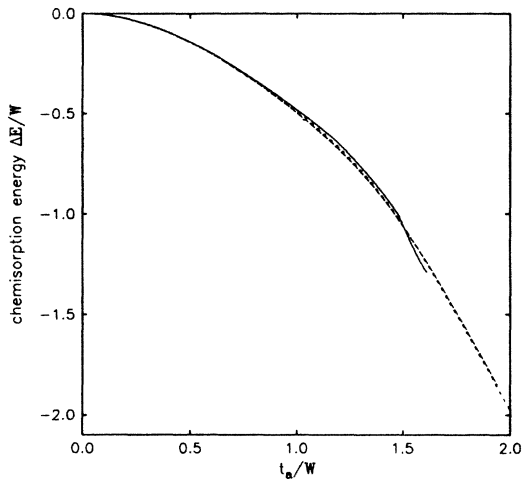

FIG. 17. The chemisorption energy in units of W as a function of t_a/W, for fcc Ni. Labeling is the same as in Fig. 2.

Our model is relatively simple. The most important limitations are the following: (1) the fact that $4s$ states in the transition metal are taken into account only implicitly (by using the screened values of the Coulomb interaction U due to $4s$ electrons, together with nonintegral occupation of the $3d$ band); (2) the Bethe-lattice approximation, which does not describe real metal surfaces properly; (3) the Hartree-Fock approximation; and (4) the $T=0$ temperature limit. Nevertheless, several correct qualitative predictions of this model (demagnetization of the surface upon chemisorption and negative charge transfer to hydrogen) support the main findings of this work.

One of the main findings of the present paper is that the restricted Hartree-Fock approach is inadequate in locating the hydrogen derived peak. An upward shift of the lowest hydrogen level, caused by an increase of the occupation of the reversely polarized spin states, and the energy decrease of the second (hydrogen affinity) level, calls for a spin-polarized correlation diagram. The present model is amenable to extensions such as including a finite temperature and phonon coupling. Usually in an *ab initio* approach, the $T=0$ description serves to determine parameters which are then fed to a model simpler than ours (e.g., the Heisenberg spin model) to find the finite temperature behavior.[7] At this stage most of the advantage of using *ab initio* methods is lost. That is why we think it is still useful to study model Hamiltonians in the theory of chemisorption.

ACKNOWLEDGMENTS

Stimulating discussions with R. E. Allen, A. B. Anderson, D. Cocke, J. E. Demuth, T. L. Einstein, G. Ertl, and D. Tomanek are gratefully acknowledged. This work was supported by the Robert A. Welch Foundation (under Grant No. A-929).

*On leave from Department of Physics, Jagellonian University, PL-30-059 Cracow, Poland.
[1]K. J. Hedvall, E. Hedin, and O. Persson, Z. Phys. Chem. B **27**, 136 (1934).
[2]H. J. Zeiger, B. Wasserman, M. S. Dresselhaus, and G. Dresselhaus, Surf. Sci. **124**, 583 (1983).
[3]M. R. Shanabarger, Phys. Rev. Lett. **43**, 1964 (1979).
[4]H. Kaarmann, H. Hoinkes, and H. Wilsch, Phys. Rev. B **30**, 424 (1984).
[5]G. Ertl and J. Rüstig, Surf. Sci. **119**, 1134 (1982).
[6]H. Robota, W. Vielhater, and G. Ertl, Surf. Sci. **136**, 111 (1984); G. Ertl, Surf. Sci. **152/153**, 328 (1985).
[7]M. Weinert and J. W. Davenport, Phys. Rev. Lett. **54**, 1547 (1985).
[8]C. Umrigar and J. W. Wilkins, Phys. Rev. Lett. **54**, 1551 (1985).
[9]T. H. Upton and W. A. Goddard, Phys. Rev. Lett. **42**, 472 (1979).
[10]M. M. Goodgame and W. A. Goddard, Phys. Rev. Lett. **48**, 135 (1982); B. Delley, A. J. Freeman and D. E. Ellis, *ibid.* **50**, 488 (1983); J. Bernholc and N. A. W. Holtzwarth, *ibid.* **50**, 1451 (1983).
[11]D. M. Newns, Phys. Rev. **178**, 1123 (1969); J. P. Muscat and D. M. Newns, Prog. Surf. Sci. **9**, 1 (1978).
[12]W. Brenig and K. Schönhammer, Z. Phys. **267**, 201 (1974).
[13]G. Doyen and G. Ertl, J. Chem. Phys. **68**, 5417 (1978).
[14]J. E. Demuth, Surf. Sci. **65**, 369 (1977).
[15]H. Conrad, G. Ertl, J. Küppers, and E. E. Latta, Surf. Sci. **58** 578 (1976).
[16]P. Norlander, S. Holloway, and J. K. Nørskov, Surf. Sci. **136**, 59 (1984).
[17]N. D. Lang and A. R. Williams, Phys. Rev. B **18**, 616 (1978).
[18]B. I. Lundqvist, O. Gunnarson, H. Hjelmberg, and J. K. Nørskov, Surf. Sci. **89**, 196 (1979).
[19]C. M. Varma and A. J. Wilson, Phys. Rev. B **22**, 3795 (1980); A. J. Wilson and C. M. Varma, *ibid.* **22**, 3805 (1980).
[20]R. C. Baetzold, Solid State Commun. **44**, 781 (1982); E. Shustorovich, J. Phys. Chem. **87**, 14 (1983).
[21]B. Bell and A Madhukar, Phys. Rev. B **14**, 4281 (1976).
[22] H. Kranz, Phys. Rev. B **20**, 1617 (1976).
[23]A. M. Oleś and K. A. Chao, Phys. Rev. B **25**, 3790 (1982); **28**, 6847 (1983).
[24]J. L. Morán-Lopéz and L. M. Falicov, Phys. Rev. B **26**, 2561 (1982).
[25]M. Landolt and M. Campagna, Phys. Rev. Lett. **39**, 568 (1977).
[26]J. Hubbard, Proc. R. Soc. London, Ser. A **276**, 238 (1963); **277**, 237 (1964); **281**, 401 (1964).
[27]L. M. Roth, *Proceedings of the International Conference on the Physics of Transition Metals, Toronto, 1977,* edited by M. J. G. Lee, J. M. Perz, and E. Fawcett (IOP, London, 1978), p. 473.
[28]S. H. Liu, Phys. Rev. B **17**, 3629 (1978).
[29]L. M. Falicov and R. H. Victora, Phys. Rev. **30**, 1695 (1984).
[30]P. N. Sen and F. Yndurain, Phys. Rev. B **13**, 4387 (1976).
[31]E. N. Economou, *Green's Functions in Quantum Physics* (Springer, Berlin, 1983), pp. 97—127.
[32]P. W. Anderson, Phys. Rev. **124**, 41 (1961).
[33]Although throughout Ref. 24 Fe with $z=8$ (bcc structure) was referred to the actual calculations corresponded to Fe with $z=12$ (fcc structure). We thank Professor Morán-Lopéz for pointing out this discrepancy.
[34]R. E. Watson and L. H. Bennett, Phys. Rev. B **18**, 6439 (1978).
[35]J. Kanamori, Prog. Theor. Phys. **16**, 275 (1963); J. Friedel and C. M. Sayers, J. Phys. (Paris) **38**, 697 (1977).
[36]J. Hubbard, Phys. Rev. B **19**, 2626 (1979).
[37]E. Antonides, C. E. Janse, and G. A. Sawatzky, Phys. Rev. B **15**, 1669 (1977); **15**, 4596 (1977).
[38]S. K. Lyo and R. Gomer, in *Interactions on Metal Surfaces,* Vol. 4 of *Topics in Applied Physics,* edited by R. Gomer (Springer, Berlin, 1975), Chap. 2.
[39]T. L. Einstein, J. A. Hertz, and J. R. Schrieffer, in *Theory of Chemisorption,* Vol. 13 of *Topics in Current Physics,* edited by J. R. Smith (Springer, Berlin, 1980), Chap. 7.
[40]H. B. Michaelson, J. Appl. Phys. **62**, 3193 (1975).
[41]J. W. Richardson, W. C. Nieuwport, R. R. Powell, and W. F. Edgell, J. Chem. Phys. **34**, 1057 (1962).
[42]M. M. Hall (private communication).
[43]G. Blyholder, J. Chem. Phys. **62**, 3193 (1975).
[44]J. P. Muscat, Surf. Sci. **110**, 389 (1981).
[45]M. C. Desjonquéres and D. Spanjaard, J. Phys. C **16**, 3389 (1983); C. Thuault-Cytermann, M. C. Desjonquéres, and D. Spanjaard, *ibid.* **16**, 5689 (1983).
[46]F. J. Himpsel, J. A. Knapp, and D. E. Eastman, Phys. Rev. B **19**, 2872 (1979).
[47]F. Greuter, I. Strathy, E. W. Plummer, and W. Eberhardt, Phys. Rev. B **33**, 736 (1986).

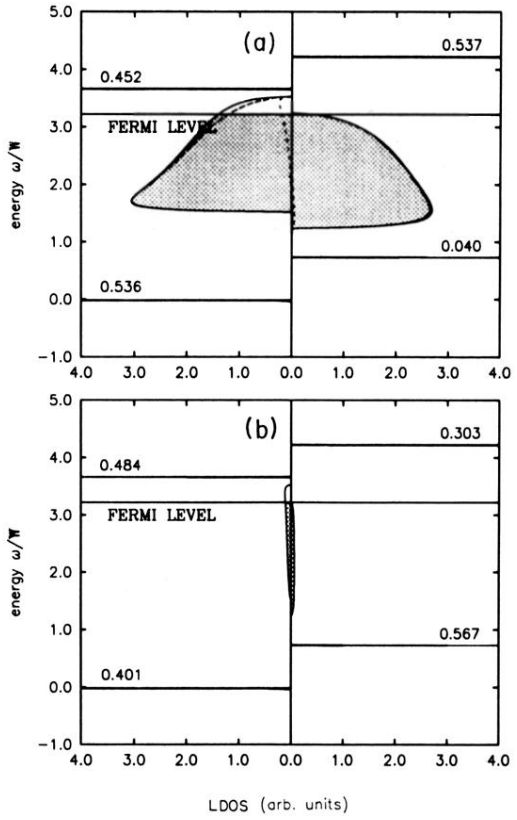

FIG. 16. The local density of states on the substrate atom (a) and on the substrate atom (b) for the "antiferromagnetic" case of fcc Ni with $t_a/W = 1.0$. Labeling is the same as in Fig. 5.

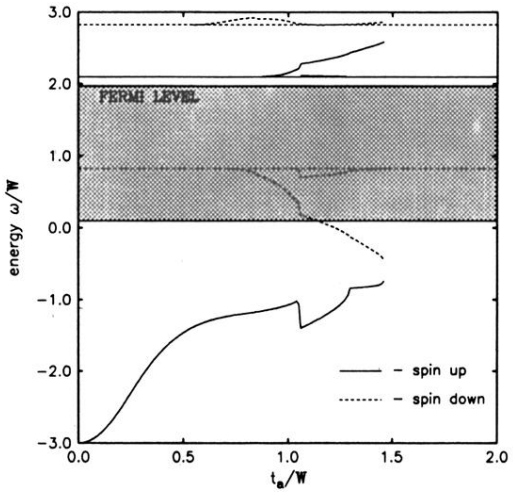

FIG. 2. The position of the localized states as a function of t_a/W for the "ferromagnetic" case of bcc Fe. Solid lines indicate spin-up states, and dashed lines spin-down states. The thick solid line is the Fermi level, whereas two pairs of thin straight lines (solid and dashed) correspond to the boundaries of the bands for spin up and spin down, respectively. The shaded region shows the occupied states.

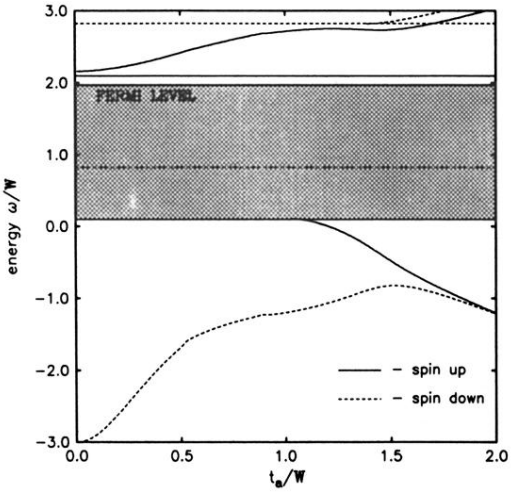

FIG. 3. The position of the localized states as a function of t_a/W for the "antiferromagnetic" case of bcc Fe. The labeling is the same as in Fig. 2.

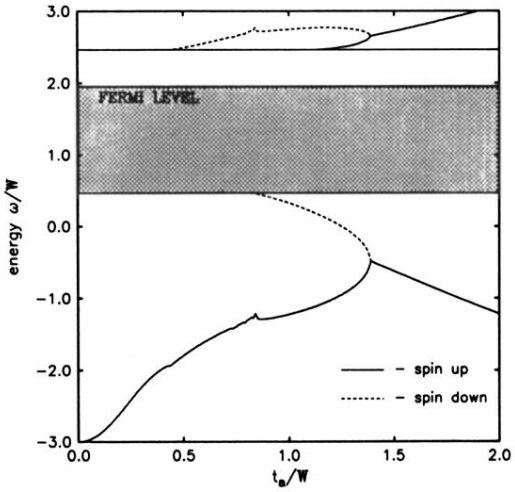

FIG. 4. The position of the localized states as a function of t_a/W for the "paramagnetic" case of bcc Fe. The labeling is the same as in Fig. 2.

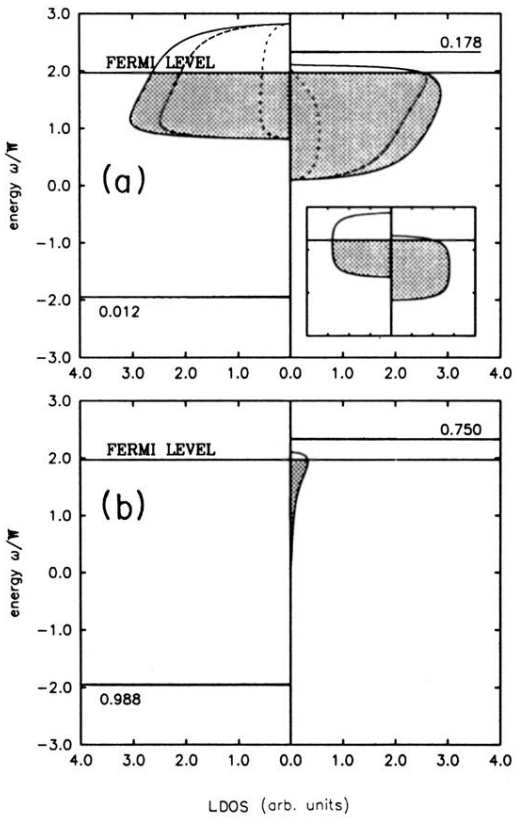

FIG. 5. The local density of states (LDOS) on the substrate atom (a) and on the adatom (b) for the "antiferromagnetic" case of bcc Fe with $t_a/W=0.4$. The thick solid line signifies the Fermi level, and the shaded region marks occupied states. Right-hand and left-hand parts of the figure correspond to up and down spins, respectively. The short-dashed line corresponds to the LDOS of orbital 1 at site 0. The long-dashed line represents the LDOS of all other d orbitals together, and the thin solid line represents the total LDOS for the site 0 crystal atom. The inset in the right corner displays the shape of the pure crystal band.

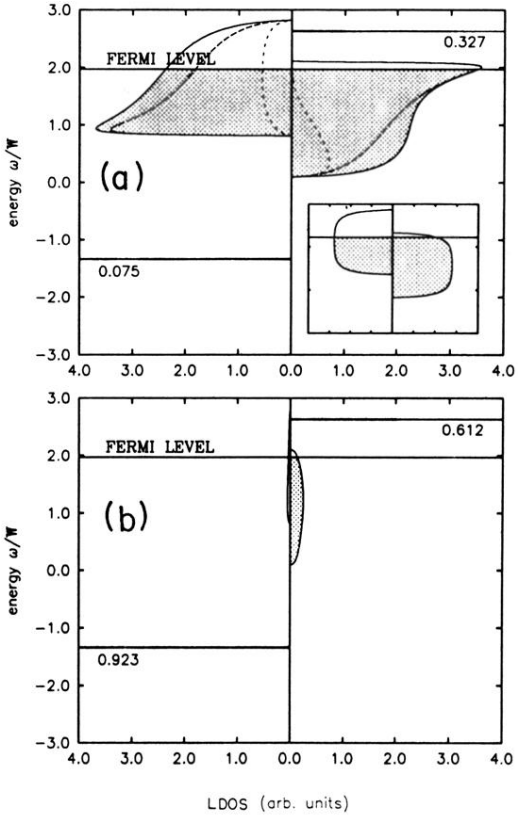

FIG. 6. The same as Fig. 5, but for $t_a/W=1.0$.

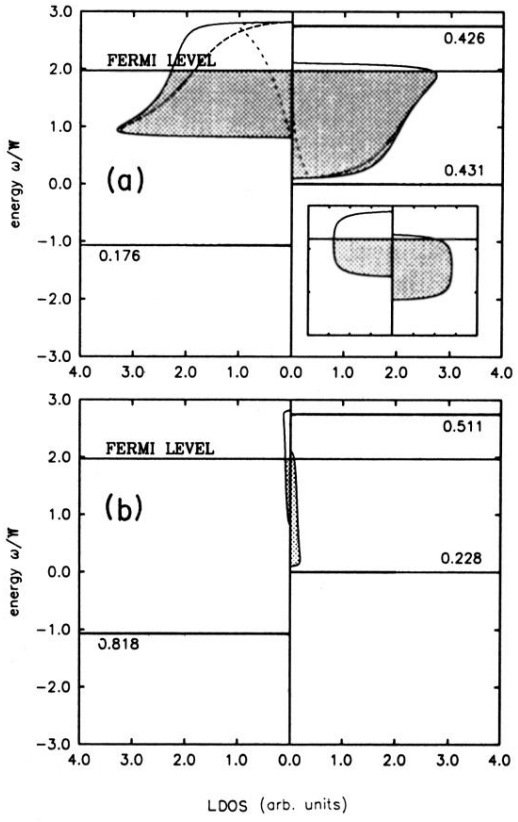

FIG. 7. The same as Fig. 5, but for $t_a/W = 1.3$.